Nuclear Engineering and Technology 48 (2016) 915–924

Available online at ScienceDirect

Nuclear Engineering and Technology

journal homepage: www.elsevier.com/locate/net

Original Article

Single Bubble Dynamic Behavior in AL_2O_3/H_2O Nanofluid on Downward-Facing Heating Surface

Yun Wang and Junmei Wu *

State Key Laboratory for Strength and Vibration of Mechanical Structures, School of Nuclear Science and Technology, Xi'an Jiaotong University, 28#, Xianning West Road, Xi'an 710049, China

ARTICLE INFO

Article history:
Received 28 September 2015
Received in revised form
6 February 2016
Accepted 11 February 2016
Available online 4 March 2016

Keywords:
Bubble Dynamics
Downward-Facing Heating Surface
Moving Particle Semi-Implicit
Nanofluid

ABSTRACT

After a severe accident to the nuclear reactor, the in-vessel retention strategy is a key way to prevent the leakage of radioactive material. Nanofluid is a steady suspension used to improve heat-transfer characteristics of working fluids, formed by adding solid particles with diameters below 100 nm to the base fluids, and its thermal physical properties and heat-transfer characteristics are much different from the conventional working fluids. Thus, nanofluids with appropriate nanoparticle type and volume concentration can enhance the heat-transfer process. In this study, the moving particle semi-implicit method-meshless advection using flow-directional local grid method is used to simulate the bubble growth, departure, and sliding on the downward-facing heating surface in pure water and nanofluid (1.0 vol.% Al_2O_3/H_2O) flow boiling processes; additionally, the bubble critical departure angle and sliding characteristics and their influence are also investigated. The results indicate that the bubble in nanofluid departs from the heating surface more easily and the critical departure inclined angle of nanofluid is greater than that of pure water. In addition, the influence of nanofluid on bubble sliding is not significant compared with pure water.

1. Introduction

In a nuclear power system, the in-vessel retention (IVR) strategy is a key technology for mitigating core melt accident and preventing the leakage of radioactive material after the core melt caused by a severe accident. Henry and Fauske [1] proposed cooling the outer surface of the pressure vessel by injecting water into the reactor chamber, a process known as external reactor vessel cooling. This is a helpful process because improving the IVR capacity will increase the IVR safety margin and relieve the consequences of core melt accident. Utilization of nanofluid, first proposed by Choi and Eastman [2] in 1995, has better heat-transfer performance and is investigated as a potential solution worldwide. Kim et al. [3] experimentally investigated Al_2O_3/H_2O nanofluid flow boiling and confirmed that the critical heat flux enhancement is 30%

* *Corresponding author.*
E-mail address: wjmxjtu@mail.xjtu.edu.cn (J. Wu).
http://dx.doi.org/10.1016/j.net.2016.02.008

with 0.1 vol.% nanoparticle volume concentration. In another study, Kim et al. [4] showed that the critical heat flux enhancement is approximately 40% to 50% for Al_2O_3/H_2O and ZnO/H_2O nanofluids (with 0.01 vol.% nanoparticle volume concentration) in the flow boiling process. Ahn et al. [5] experimentally studied the critical heat flux of Al_2O_3/H_2O with 0.01 vol.% concentration; in their study, compared with pure water, the critical heat flux enhancement was 24% for 1 m/s velocity and 40% for 4 m/s velocity. For the microchannel, Vafaei and Wen [6] researched the flow boiling process of Al_2O_3/H_2O nanofluid. Their study results showed that the nanofluid critical heat flux enhancement was 51% for 0.1 vol.% concentration. Xu and Xu [7] reported that nanoparticle deposition was not found during the flow boiling heat-transfer process. In addition, the coalescence and fragmentation of bubbles in pure water were found to be random and confused. Nevertheless, the flow instability of nanofluid (0.2 vol.%, and 40 nm nanoparticle diameter, Al_2O_3/H_2O) was found to show an obvious decline. Buongiorno et al. [8] investigated the IVR capacity of nanofluids, and reported that the increase in decay power removal through the vessel using a nanofluid (0.1 vol.%, Al_2O_3/H_2O) was approximately 40%. In the IVR strategy, accelerating the bubble sliding and departure are very important, because if the bubble adheres to the heating surface and becomes gas film, the heat transfer will deteriorate. Thus, it is important to maintain the integrity of the reactor vessel. In these days, a number of papers on experimental and theoretical investigations of nanofluid boiling heat transfer are being published.

It is well-known that the steam bubble departs from the downward-facing heating surface with more difficultly with increasing inclined angle. To implement the IVR strategy, it is thus very important to know whether the bubble can depart from the downward-facing heating surface. If the answer is positive, new working fluid can replenish the area where the bubble used to be. Thus, the IVR capacity is increased with increasing the critical inclined angle of the bubble. However, so far, only a few studies on the bubble dynamic behavior in nanofluids and pure water on the downward-facing heating surface have been presented. In this study, the moving particle semi-implicit method-meshless advection using flow-directional local grid (MPS-MAFL) method is used to simulate the growth, departure, and sliding of the bubble on the downward-facing heating surface in pure water and nanofluid (1.0 vol.% Al_2O_3/H_2O) flow boiling processes. In addition, the bubble critical departure angle and sliding characteristics and their influence were also investigated.

2. Numerical Simulation Method

The conventional numerical method is based on the Eulerian coordinate system, and it is unqualified to simulate the interface with severe deformation, because all the information about the field is assigned in the grid. However, because the interface is too small, the grid size needs to be smaller as well. This makes the simulation burdensome owing to the complexity involved the calculation steps. Koshizuka and Oka [9] proposed a new meshless method to track this change, and called it the *moving particle semi-implicit method* (MPS), which is based on the Lagrangian coordinate system. However, a large number of particles need to be traced in the Lagrangian coordinate system under the inlet and outlet conditions. Thus, there is a need for a computer with significantly higher calculation capacity in terms of memory and speed. Yoon et al. [10,11] presented an improved MPS method by using the MPS-MAFL method to analyze the complex moving interface problem with inlet and outlet flows. Compared with MPS, MPS-MAFL has two more steps: one is the relocation of the particles and the other is Eulerian calculation, where it makes the number of particles traced smaller and improves the calculation efficiency. The governing equations are as follows:

$$\frac{\partial \rho}{\partial t} + \nabla \cdot (\rho \mathbf{u}) = 0 \tag{1}$$

$$\rho\left[\frac{\partial \mathbf{u}}{\partial t} + (\mathbf{u} - \mathbf{u}^c)\cdot\nabla \mathbf{u}\right] = -\nabla P + \nu \nabla^2 \mathbf{u} + \sigma\kappa \cdot \mathbf{n} + \rho g \cos\varphi \tag{2}$$

$$\frac{\partial T}{\partial t} + (\mathbf{u} - \mathbf{u}^c)\cdot\nabla T = \alpha \nabla^2 T \tag{3}$$

where $\mathbf{u}$ is the particle velocity; $\mathbf{u}^c$ represents the motion of a computing point, which is adaptively configured during the calculation; κ is the interfacial curvature, and its value is 0 for the particle that is not on the interface, so that the momentum equation corresponds to the conventional ones; φ is the inclined angle, whose value is 0 when the heating surface is vertical; however, its value is 90° when the heating surface is horizontally downward. In this method, all deferential operators appearing in the governing equation are replaced by the particle interaction model, and the weight function and models can be found in Yoon's paper [10,11]. In this work, the objective is to investigate the bubble dynamic behavior under atmospheric pressure. Because the temperature change is not significant, all the thermal physical properties are given as a constant value by an input file. All the properties are used as a constant coefficient in the governing equation, including density, specific heat, thermal conductivity, dynamic viscosity, surface tension coefficient, and thermal diffusivity. Appendix 1 shows all the notations used in this paper.

2.1. *Heat- and mass-transfer model*

In the IVR strategy, the lower head of the pressure reactor vessel (PRV) is flooded in the coolant (Fig. 1). The radius of lower head of the PRV is 2,000 mm, and the bubble diameter during sliding and departure on the heating surface is approximately 2 mm under the atmospheric pressure. Thus, according to the study by Xu et al. [12] and Maity [13], the bubble diameter is very small compared with the radius of the PRV lower head. Therefore, it is reasonable to simplify the PRV lower head outer surface into a flat heating surface with different inclined angles in the bubble dynamic behavior investigation. In this study, the bubble growth, departure, and sliding on the downward-facing heating surface in pure water and nanofluid flow processes are simulated. Fig. 2 shows the dimensional numerical simulation area (size 35 mm × 20 mm). In this figure, the blue particles indicate pure water or nanofluid, the green particles indicate the wall, and the black particles are the

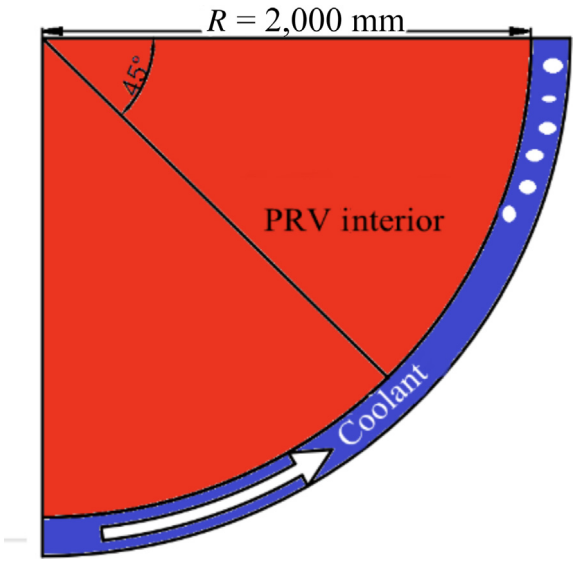

Fig. 1 – Lower head plate model. PRV, pressure reactor vessel.

heating surface. The layout of the computational particles for 45° inclined angle is also shown in Fig. 2.

During the process of bubble growth and sliding, the bubble interior force balance model can be described by Eq. (4) and Fig. 3. As the $d\theta$ is the equivalent infinitesimal of $\sin d\theta$, Eq. (4) can be simplified as Eq. (5). The heat- and mass-transfer model of the bubble on the downward-facing heat surface is shown in Eq. (6) and Fig. 4. The initial bubble diameter is 0.2 mm, and it is located 7 mm away from the inlet. Nonslip conditions were applied at the wall and heating surface.

$$P_g r d\theta L - P_l r d\theta L = \sigma \sin d\theta L \tag{4}$$

$$P_g - P_l = \frac{\sigma}{r} \tag{5}$$

$$\Delta V = \frac{Q_l + Q_g}{h_{fg}\rho_g} \tag{6}$$

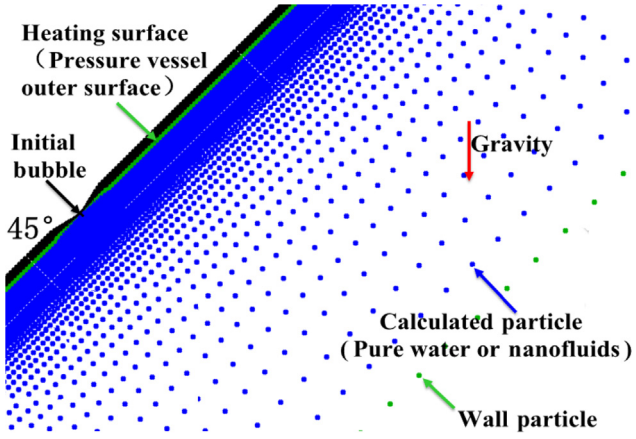

Fig. 2 – Initial shape of the bubble and layout of the particles for the 45° inclined angle.

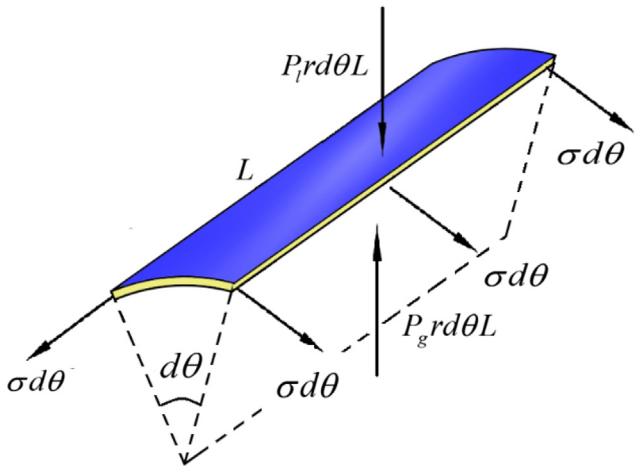

Fig. 3 – Two-dimensional balance model of the bubble interior force.

2.2. *MPS-MAFL validation*

To validate the numerical simulation results of the bubble growth and departure processes in the flow boiling process on the downward-facing heating surface, the bubble growth and sliding in pure water on the downward-facing heating surface for 45° inclined angle from Maity's experiment [13] are numerically simulated under the condition of atmospheric pressure. The initial diameter of the bubble is 0.2 mm, and the coolant is pure water with 375.15 K temperature, the wall superheat is 5.5 K, the coolant inlet subcooling temperature is 0.6 K, and the inlet velocity is 0.074 m/s. Maity [13] also investigated the contact angle of bubble under the same

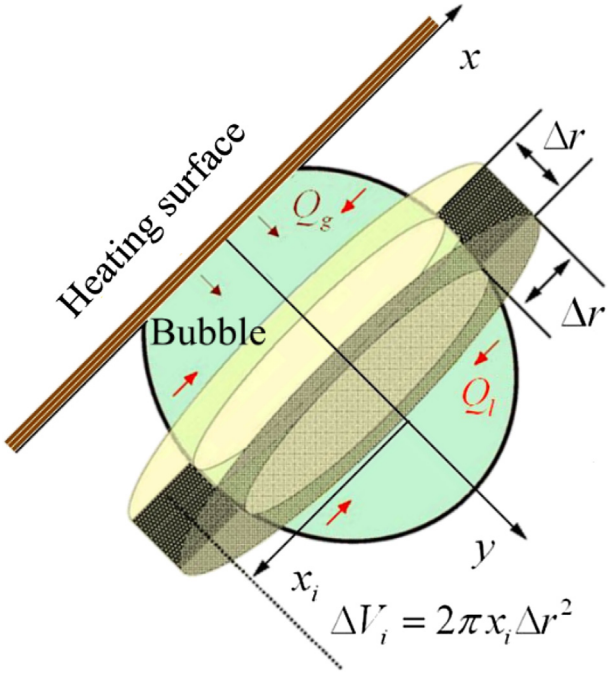

Fig. 4 – Heat- and mass-transfer model of the bubble for the 45° inclined angle.

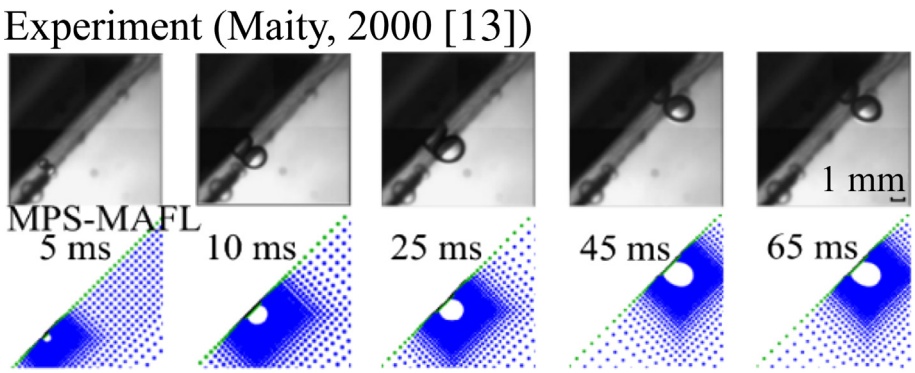

Fig. 5 – Bubble shape in the growth and sliding processes. MPS-MAFL, moving particle semi-implicit method-meshless advection using flow-directional local grid.

condition. The results show that the upstream and downstream contact angles are 50° and 40°, respectively, and the two contact angles do not significantly change in the whole process of bubble sliding. Thus, we chose a constant contact angle value of 45° for the whole growth and sliding processes. Figs. 5–7 show the numerical and experimental results of the bubble shape, diameter, and sliding velocity in the growth and sliding processes. In addition, we calculated the average relative error, the average relative absolute error, and standard deviation between the experimental data and numerical results, and their values are presented in Table 1. As can be seen, the numerical results agree with the experimental results. Thus, we were convinced that the MPS-MAFL method can reliably simulate the bubble growth, departure, and sliding processes in the flow boiling process on the downward-facing heating surface.

3. Results and discussion

3.1. *Bubble departure critical inclined angle*

In the IVR strategy, the melt decay heat in the PRV may make the coolant boil on the heating surface, and the different locations on the outer surface of the PRV correspond to the different inclined angles. It is important to know whether the bubble can depart from the heating surface, as it significantly influences the capacity of IVR. There should be a critical inclined angle beyond which the bubble can or cannot depart from the heating surface. Because the inclined angle is less than the critical inclined angle, the bubble can depart from the heating surface and the new coolant can replenish the area where the bubble used to be, following which the PRV can be cooled effectively. By contrast, if the inclined angle is greater than the critical inclined angle, the bubble cannot depart from the heating surface and becomes a gas film that adheres to the heating surface. Thus, the heat transfer is deteriorated. The factors influencing critical inclined angle are wall superheat, fluid inlet subcooling, and fluid velocity, The computational conditions are presented in Table 2. The thermal/physical property models of the Al_2O_3/H_2O nanofluid are presented in Wang and Wu's paper [14], and the related data are presented in Table 3. In this work, we have studied the bubble dynamic behavior in the Al_2O_3/H_2O nanofluid (0.1 vol.%) and pure water under atmospheric pressure. Because the temperature change is not significant, all the thermal physical properties are given as a constant value.

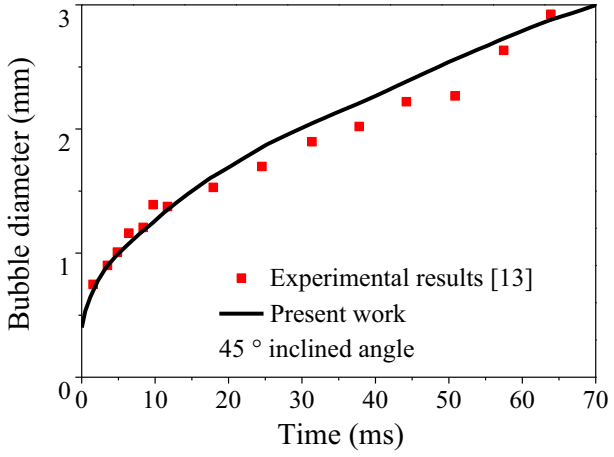

Fig. 6 – Bubble diameter in the growth and sliding processes.

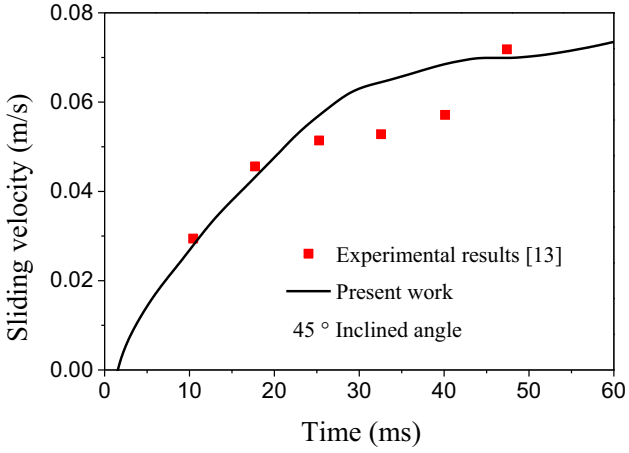

Fig. 7 – Bubble sliding velocity in the growth and sliding processes.

Table 1 – Error analysis for the experimental data and numerical results.

Index	Diameter	Sliding velocity
Average relative error (%)	−1.845	−4.300
Average relative absolute error (%)	5.695	7.863
Standard deviation	0.126	0.044

Table 2 – Computational conditions.

Case	Computational condition		
	Wall superheat (K)	Fluid subcooling (K)	Fluid velocity (m/s)
1	5.5	0.6	0.074
2	8.9	0.6	0.074
3	5.5	1.2	0.074
4	5.5	0.6	0.145

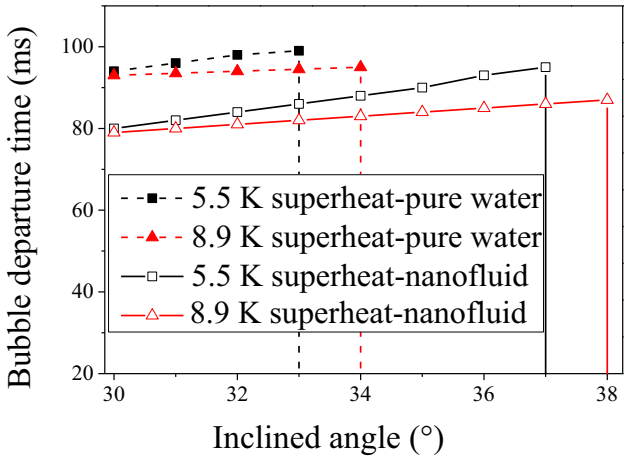

Fig. 8 – Bubble departure time from the heating surface for different superheat.

3.1.1. *Wall superheat*

The heating surface superheat has a major influence on the bubble growth rate, which affects the bubble dynamic behaviors, such as departure and sliding. Figs. 8 and 9 show the bubble departure time for different inclined angles and the bubble diameter in the heating process for the 30° inclined angle under the condition of different wall superheat (Cases 1 and 2). As shown in Fig. 8, the component perpendicular to the heating surface of buoyancy is increased with the increasing inclined angle, which makes the bubble adhere to the wall more easily, thereby increasing the departure time. By contrast, the departure time is decreased with increasing wall superheat because the bubble grows faster in this case (Fig. 9). In addition, the critical inclined angle of the bubble in nanofluid is greater than that of pure water; in Case 1, the critical inclined angle is 37° in nanofluid and 33° in pure water. In Fig. 10, the area of bubble departure in pure water and nanofluid is differentiated clearly. It can be seen that the allowable area of bubble formation in nanofluid is greater than that of pure water; in other words, the nanofluid can increase the safety margin of IVR and thereby increase the PRV cooling capacity.

3.1.2. *Fluid inlet subcooling*

Similar to the influence of wall superheat, the fluid inlet subcooling also has an influence on the bubble growth rate. Figs. 11 and 12 show the bubble departure time for different inclined angles and the bubble diameter in the heating process for 30° inclined angle under the inlet subcooling condition with different fluids (Cases 1 and 3). As shown in Fig. 11, the bubble departs from the surface with increased difficultly because the component perpendicular to the heating surface of the buoyancy is increased due to the increased inclined angle. By contrast, the departure time is increased with decreasing fluid inlet subcooling and so is the critical inclined angle. This is because the bubble in the greater subcooling fluid grows slower than that of the less subcooling fluid, as Fig. 12 shows. The main factors influencing bubble departure are gravity, buoyancy, shear force, and surface tension (Fig. 13). The component perpendicular to the heating surface of the buoyancy (F_B^n) and the surface tension (F_{st}) are resistive forces to bubble departure, whereas the component perpendicular to the heating surface of the gravity (F_G^n) and the shear force (F_τ^n) are the assistive forces to bubble departure. In the fluid with 1.2-K inlet subcooling, as the bubble is cooling and atrophy is near the main flow field, the radius of curvature of the bubble is increased, and the surface tension is decreased. This is the reason why the bubble departure from the heating surface is earlier when the fluid subcooling temperature is 1.2 K. It can be seen that the bubble growth is limited by

Table 3 – Properties of water-based alumina nanofluid with 0.1 vol.% nanoparticle concentration and 0.1 MPa pressure.

Property	Correlation	Nanofluid	Pure water	Unit
Density	$\rho_{nf} = \rho_p\phi + \rho_f(1-\phi)$	9.885×10^2	9.584×10^2	kg/m^3
Specific heat at constant pressure	$c_{p,nf} = \frac{(1-\phi)\rho_f c_{pf} + \phi\rho_p c_{pp}}{(1-\phi)\rho_f + \phi\rho_p}$	4.212×10^3	4.220×10^3	J/kg/K
Thermal conductivity	$\frac{k_{nf}}{k_f} = 1 + 4.4\mathrm{Re}^{0.4}\mathrm{Pr}^{0.66}\left(\frac{T}{T_{fr}}\right)^{10}\left(\frac{k_p}{k_f}\right)^{0.03}\phi^{0.66}$	7.841×10^{-1}	6.830×10^{-1}	W/m/K
Dynamic viscosity	$\mu_{nf} = \mu_f(T)/[1 - 34.87(d_p/d_f)^{-0.3}\phi^{1.03}]$	2.972×10^{-4}	2.825×10^{-4}	Pa·s
Surface tension coefficient	$\frac{\sigma_{f0} - \sigma_{nf}}{\sigma_{f0}} = b\ln\left(\frac{\phi}{a} - 1\right)$	6.319×10^{-2}	5.892×10^{-2}	N/m
Thermal diffusivity	$\alpha_{nf} = k_{nf}/(\rho_{nf}c_{pnf})$	1.884×10^{-7}	1.690×10^{-7}	m^2/s
Prandtl number	$\mathrm{Pr}_{nf} = \mu_{nf}/(\rho_{nf}\alpha_{nf})$	1.478×10^0	1.950×10^0	1

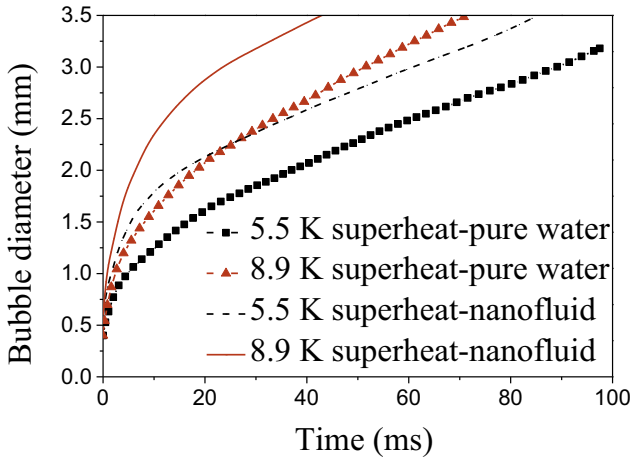

Fig. 9 – Bubble diameter for the 30° inclined angle (wall superheat).

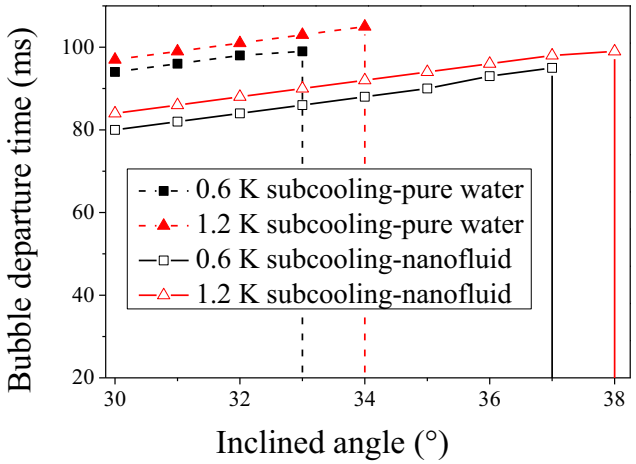

Fig. 11 – Bubble departure time from the heating surface for different subcooling.

increasing the fluid subcooling. Thus, the critical inclined angle will be decreased. Therefore, the optimal value needed to make the critical inclined angle maximum is worth investigating. In addition, the critical inclined angle of the bubble in nanofluid is greater than that in pure water, suggesting that the allowable area of bubble originating in the nanofluid is greater than that of pure water; additionally, the safety margin of IVR is increased to enhance the PRV cooling capacity when using nanofluid as the working fluid.

3.1.3. *Fluid velocity*

The fluid velocity has an influence not only on the flow field, which affects the bubble growth rate, but also on the shear force, which affects the bubble dynamic behaviors such as departure and sliding. Figs. 14 and 15 show the bubble departure time for different inclined angles and the bubble diameter in the heating process for 30° inclined angle under the condition of different fluid velocities (Cases 1 and 4). As shown in Fig. 14, the component perpendicular to the heating surface of the buoyancy increases with the increase in the inclined angle, making the bubble to adhere to the wall more easily and increasing departure time. By contrast, the departure time decreases and critical inclined angle increases with increasing fluid velocity because the bubble grows faster with greater fluid velocity (Fig. 15). This is because the disturbance in the fluid is more intense for the case of greater velocity. The relative movement between interface and fluid is also improved. Thus, the interface heat transfer is enhanced. Moreover, as analyzed in Fig. 13, the component perpendicular to the heating surface of the shear force is also increased with increasing fluid velocity. This makes the bubble depart from the heating surface more easily. Compared with pure water, the critical inclined angle is greater in nanofluid. This difference can be explained as follows: as the bubble grows and touches the subcooling fluid, the front portion of the bubble will start to condense. It is due to this phenomenon, the heat transfer in nanofluid is more intense than that in pure water, and the bubble condensation in nanofluid is more significant. Thus, the interface curvature in nanofluid is less than that in pure water as shown in Fig. 13. As a result, the

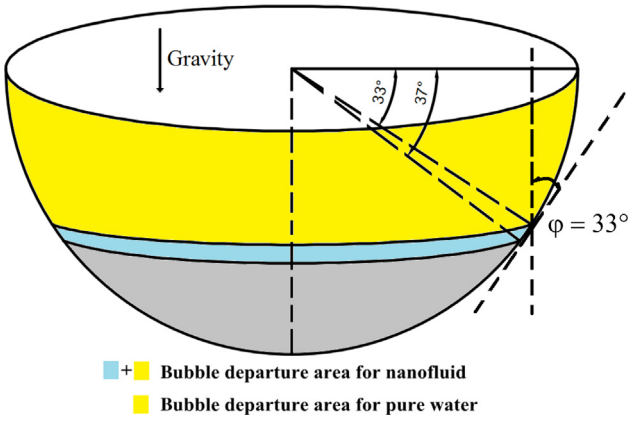

Fig. 10 – Schematic of the area for bubble departure from the lower head surface in pure water and nanofluid for Case 1.

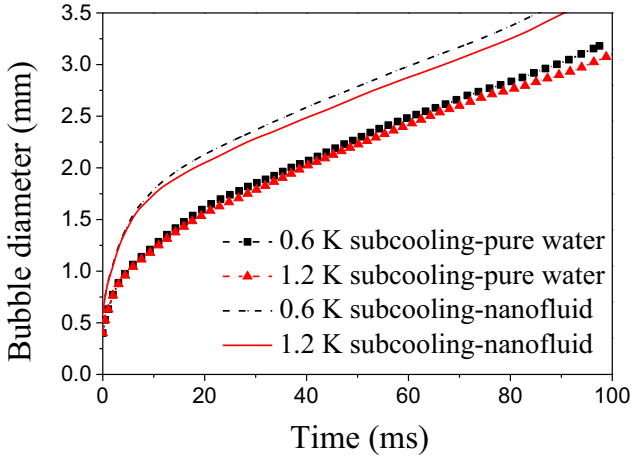

Fig. 12 – Bubble diameter for the 30° inclined angle (fluid subcooling).

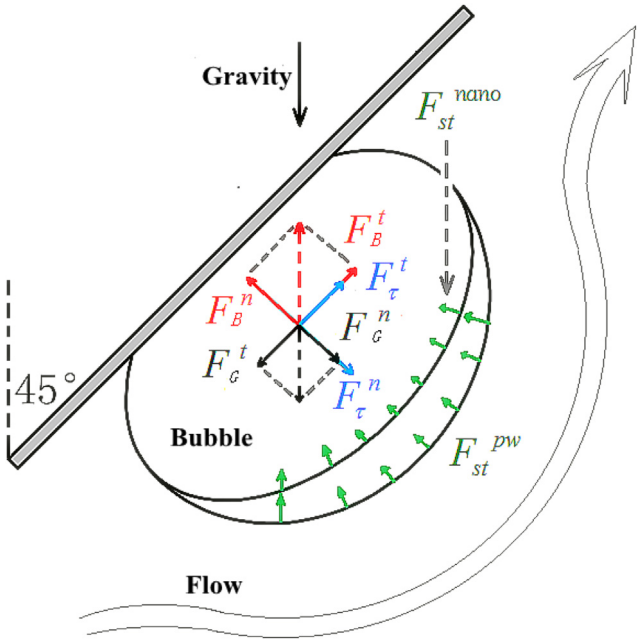

Fig. 13 – Schematic of bubble exterior force analysis for the 45° inclined angle. In the figure, superscripts *t* and *n* are the parallel and perpendicular components; superscripts nano and *pw* are the two surface tensions with two kinds of radius of curvature; subscripts *G*, *B*, *st*, and τ represent gravity, buoyancy, surface tension, and shear force.

surface tension is decreased. By contrast, the component perpendicular to the heating surface of the shear force is greater in nanofluid as the dynamic viscosity of nanofluid is greater. This finding is consistent with the experimental results of Xu et al. [12], who reported that the bubble cannot depart from the heating surface, but can slide onto the heating surface in pure water. However, the bubble in nanofluid can depart from the heating surface for the condition presented in Case 4. This finding is useful to understand the nanofluid bubble dynamic behavior and is worth studying in future studies. Similar to the influence of wall superheat and fluid

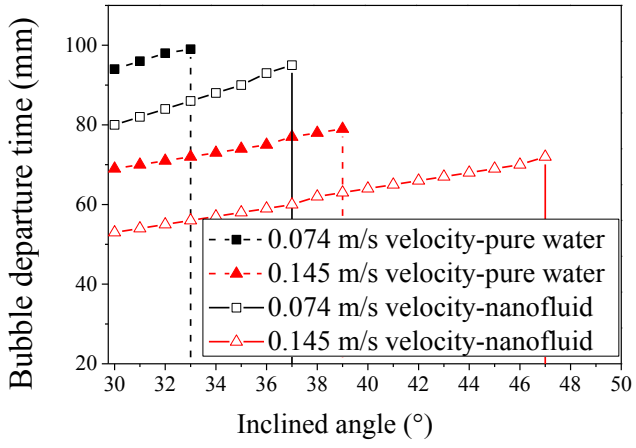

Fig. 14 – Bubble departure time from the heating surface for fluid velocity.

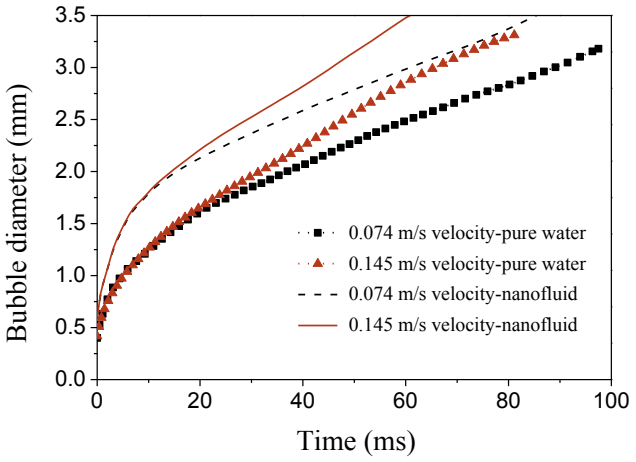

Fig. 15 – Bubble diameter for the 30° inclined angle (fluid velocity).

inlet subcooling, nanofluid can enhance heat transfer to improve the capacity of IVR. According to the study by Kwark et al. [15], it can be predicted that the bubble in nanofluid departs more easily from the heating surface. Because the authors of that study [15] qualitatively presented that the contact angle of the bubble in nanofluid is smaller than that in pure water, the component perpendicular to the heating surface of shear force is greater and the surface tension is small. In this case, the bubble departure critical slant angle in nanofluid should be increased. In other words, the nanofluid can enhance the IVR capacity from the viewpoint of bubble dynamic behavior. Actually, this enhancement may be more than the value mentioned earlier.

3.2. *Bubble sliding*

The bubble sliding on the heating surface is a much important part of bubble dynamic behavior; however, studies on bubble sliding are scarce in the literature. Under the condition that a bubble cannot depart from the downward-facing heating surface, the bubble sliding is expected to enhance the heat-

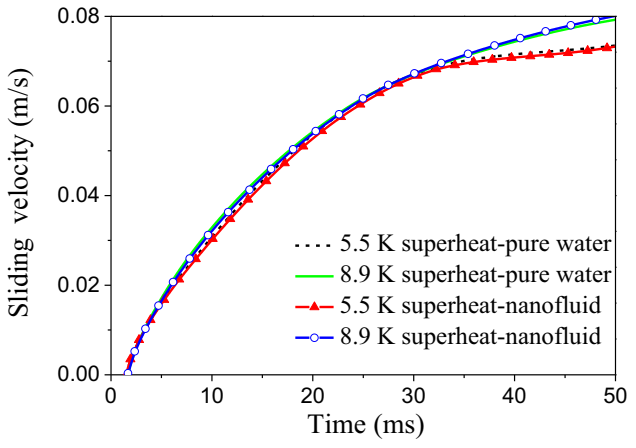

Fig. 16 – Bubble sliding velocity in the growth and sliding processes for the 30° inclined angle (wall superheat).

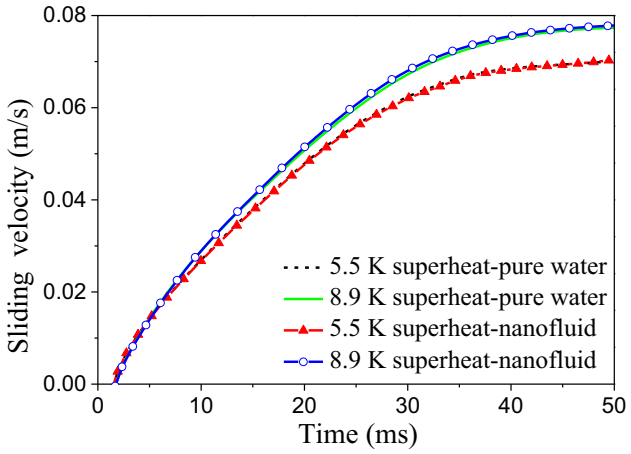

Fig. 17 – Bubble sliding velocity in the growth and sliding processes for the 45° inclined angle (wall superheat).

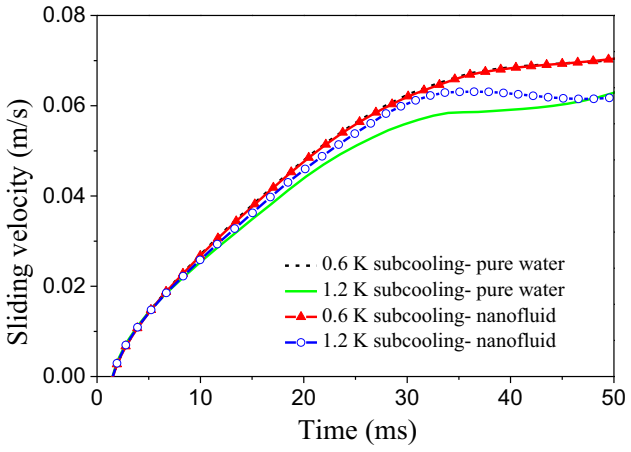

Fig. 19 – Bubble sliding velocity in the growth and sliding processes for the 45° inclined angle (fluid inlet subcooling).

transfer process because the new working fluid replenishes the previous position of the bubble. This is a key supplement to the heat transfer when the bubble cannot depart from the heating surface. Similar to the bubble departure critical inclined angle, the main factors influencing bubble sliding are wall superheat, fluid inlet subcooling, and velocity.

3.2.1. *Wall superheat*

As shown in Figs. 16 and 17, the bubble sliding velocity is greater under the condition of greater wall super heat (Cases 1 and 2) because the bubble grows faster in the case of higher wall superheat. Then, the buoyancy, gravity, and shear force are increased by increasing the bubble volume for the greater wall superheat. As is analyzed in Fig. 13, the component parallel to the heating surface of the buoyancy (F_B^t) and the shear force (F_τ^t) are the assistive forces to bubble sliding, whereas the component parallel to the heating surface of the gravity (F_G^t) is the resistive force to bubble sliding. Compared with the condition of 30° inclined angle, the bubble velocity changes are greater in pure water and nanofluid for different heating surface wall superheat for the 45° inclined angle condition. This is because the influence of shear force is greater than that of buoyancy for the greater inclined angle. The bubble in nanofluid grows faster than that in pure water and this is explained in the previous section; however, the bubble sliding velocity in nanofluid is no different from the bubble sliding velocity in pure water. This is because the shear force is the major factor influencing the bubble sliding. However, due to the faster bubble growth, the shear force difference is very small.

3.2.2. *Fluid inlet subcooling*

Figs. 18 and 19 show that the bubble slides slowly under the condition of greater fluid inlet subcooling (Cases 1 and 3). Under the aforementioned condition, the bubble grows more slowly in the case of greater fluid subcooling. Thus, the buoyancy, gravity, and shear force are all decreased by decreasing the bubble volume for the greater wall superheat. Compared with the condition of 45° inclined angle, the bubble velocity changes are greater in pure water and nanofluid for different fluid inlet subcooling for the 30° inclined angle, which explains why the influence of buoyancy is greater for

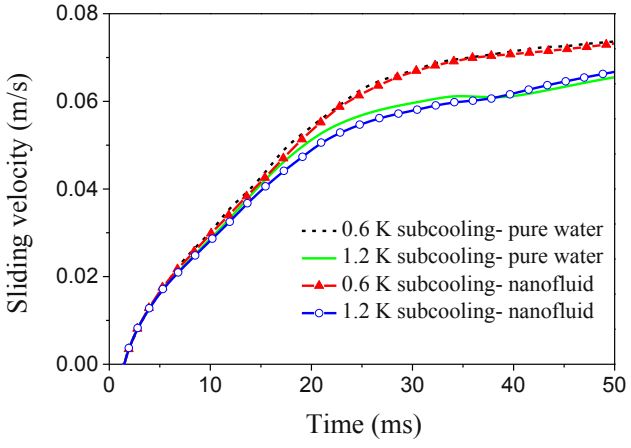

Fig. 18 – Bubble sliding velocity in the growth and sliding processes for the 30° inclined angle (fluid inlet subcooling).

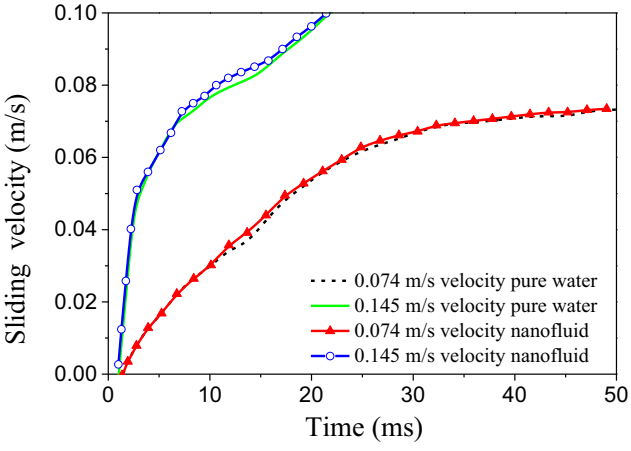

Fig. 20 – Bubble sliding velocity in the growth and sliding processes for the 30° inclined angle (fluid velocity).

the smaller inclined angle. For this influence factor, the bubble sliding velocity in nanofluid is no different from the bubble sliding velocity in pure water. It is also due to the difference of shear force is very small for the conditions of grow faster or more slowly.

3.2.3. *Fluid velocity*

Compared with the condition of different wall superheat and fluid inlet subcooling, the influence of fluid velocity on the bubble sliding velocity is more remarkable as shown in Figs. 20 and 21 (Cases 1 and 4). Because the component parallel to the heating surface of the buoyancy and the shear force are the assistive forces to bubble sliding, the bubble sliding velocities in the case of 0.145 m/s fluid velocity are greater than that of the 0.074 m/s fluid velocity. In addition, when the bubble sliding velocity is increased to the value of fluid velocity (the bubble sliding velocity is close to 0.072 m/s and the fluid velocity is 0.074 m/s at 50 ms), the relative velocity between the bubble and fluid is reduced. As a result, the shear force is reduced. The component parallel to the heating surface of the shear force will thus become the resistive force to bubble sliding, and the bubble sliding velocity is greater than the fluid velocity. At this point, the bubble is accelerated only by the component parallel to the heating surface of the buoyancy, until the shear force is great enough to balance the bubble with the other forces. As we know, the bubble will be accelerated by the buoyancy until the forces (buoyancy, gravity, and shear force) balance. Because the calculated load is not enough in the present work, the bubble slides out of the computational area when the bubble sliding velocity is near the fluid velocity. Thus, the bubble is accelerated only by the component parallel to the heating surface of the buoyancy. However, it can be predicted that the bubble will accelerate continually until the shear force is great enough to reach a new equilibrium with gravity and buoyancy. As mentioned earlier, the bubble sliding velocities in pure water and nanofluid have no difference. This is because the major factor influencing bubble sliding is the component parallel to the shear force, and the component parallel to the shear force change, which is caused by the very small heat-transfer difference between pure water and nanofluid. Thus, the influence of nanofluid on bubble sliding is not significant.

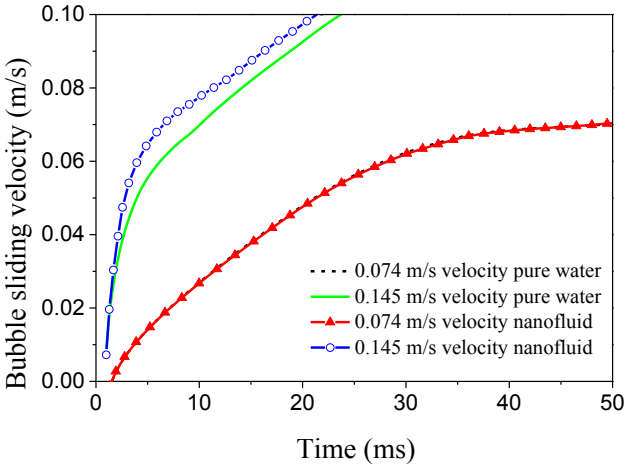

Fig. 21 – Bubble sliding velocity in the growth and sliding processes for the 45° inclined angle (fluid velocity).

4. Conclusions

In this study, the MPS-MAFL method was used to simulate the bubble growth, departure, and sliding on the downward-facing heating surface in pure water and nanofluid (1.0 vol.% Al_2O_3/H_2O) flow processes. In addition, we also investigated the critical departure angle of bubble and bubble sliding characteristics and their influence. The key findings of our study are as follows:

(1) The bubble departs from the heating surface more easily in the case of greater wall superheat and fluid velocity. The influence of fluid inlet subcooling on the bubble departure is not unilateral. In this study, the inlet subcooling was in the range of 0.6–1.2 K. The bubble in the coolant with 1.2-K subcooling departs from the heating surface more easily. Compared with wall superheat and fluid inlet subcooling, the fluid velocity has a major influence on the bubble departure.
(2) Under the same condition, the bubble in the Al_2O_3/H_2O nanofluid departs from the heating surface earlier. This illustrates that using the Al_2O_3/H_2O nanofluid to cool the PRV outer surface in the IVR strategy can supplement the new coolant to ensure bubble departure on time before the bubble becomes a gas film. Thus, the outer surface of the PRV can be cooled effectively, and eventually the capacity of IVR is improved.
(3) The shear force is important for the bubble dynamic behaviors such as growth, sliding, and departure. The critical inclined angle in the Al_2O_3/H_2O nanofluid is greater than that in pure water, which confirms that using the Al_2O_3/H_2O nanofluid to cool the PRV outer surface in the IVR strategy can increase the allowable area of bubble birthing, thereby increasing the safety margin of IVR.
(4) For bubble sliding, the shear force change caused by the heat-transfer difference between pure water and nanofluid is very small. Fluid velocity is the main influencing factor, compared with wall superheat and fluid inlet velocity. However, the influence of nanofluid on bubble sliding is not significant on downward-facing heating surface.

Conflicts of interest

The author declares no conflicts of interest.

Acknowledgments

This work was supported by the National Natural Science Foundation of China (No. 51276164) and the Open Fund Program of the Key Laboratory of Advanced Reactor Engineering and Safety, Ministry of Education of China.

Appendix 1. Nomenclature.

c_p	Specific heat at constant pressure (kJ/kg·K)
d	Diameter (m)
h_{fg}	Latent heat(J/kg)
L	Length (m)
M	Relative molecular weight
n	Unit normal vector
N	Avogadro constant
P	Pressure (Pa)
Pr	Prandtl number
Q	Heat (J)
r	Radius (m)
Re	Reynolds number
t	Time (seconds)
T	Temperature (K)
V	Volume (m^3)
u	Velocity (m/s)
P	Density of nanofluid (kg/m^3)
υ	Dynamic viscosity (kg/m·s)
σ	Surface tension (N/m)
κ	Curvature (1/m)
α	Thermal diffusivity (m^2/s)
δ	Heat conductivity thickness (m)
φ	Inclined angle (degrees)
θ	Angle (degrees)
Superscripts	
pw	Bubble surface in pure water
nano	Bubble surface in nanofluid
n	Normal direction
t	Tangential direction
Subscripts	
0	Normal temperature of 293.15 K
B	Buoyancy
f	Base fluid
f0	Standard state of atmospheric pressure and 273.15 K in temperature
fr	Standard of freezing point
g	Gas phase
G	Gravity
l	Liquid phase
nf	Nanofluids
P	Particle
St	Surface tension
τ	Shear force

REFERENCES

[1] R.E. Henry, H.K. Fauske, External cooling of a reactor vessel under severe accident conditions, Nucl. Eng. Des. 139 (1993) 31–43.

[2] S.U.S. Choi, J.A. Eastman, Enhancing thermal conductivity of fluids with nanoparticles, in: International Mechanical Engineering Congress and Exhibition, San Francisco, CA, 1995, pp. 99–106.

[3] S.J. Kim, L.W. Hu, T. McKrell, Alumina nanoparticles enhance the flow boiling critical heat flux of water at low pressure, J. Heat Transfer 130 (2008) 044501–044503.

[4] S.J. Kim, T. McKrell, J. Buongiorno, Experimental study of flow critical heat flux in alumina-water, zinc-oxide-water, and diamond-water nanofluids, J. Heat Transfer 131 (2009) 043204–043210.

[5] H.S. Ahn, H. Kim, H.J. Jo, Experimental study of critical heat flux enhancement during forced convective flow boiling of nanofluid on a short heated surface, Int. J. Multiphase Flow 36 (2010) 375–384.

[6] S. Vafaei, D. Wen, Critical heat flux (CHF) of subcooled flow boiling of alumina nanofluids in a horizontal microchannel, J. Heat Transfer 132 (2010) 102–404.

[7] L. Xu, J. Xu, Nanofluid stabilizes and enhances convective boiling heat transfer in a single microchannel, Int. J. Heat Mass Transfer 55 (2012) 5673–5686.

[8] J. Buongiorno, L.W. Hu, G. Apostolakis, A feasibility assessment of the use of nanofluids to enhance the in-vessel retention capability in light-water reactors, Nucl. Eng. Des. 239 (2009) 941–948.

[9] S. Koshizuka, Y. Oka, Moving-particle semi-implicit method for fragmentation of incompressible fluid, Nucl. Sci. Eng. 123 (1996) 421–434.

[10] H.Y. Yoon, S. Koshizuka, Y. Oka, A mesh-free numerical method for direct simulation of gas-liquid phase interface, Nucl. Sci. Eng. 133 (1999) 192–200.

[11] H.Y. Yoon, S. Koshizuka, Y. Oka, Direct calculation of bubble growth, departure, and rise in nucleate pool boiling, Int. J. Multiphase Flow 27 (2001) 277–298.

[12] J.J. Xu, W.B. Zhou, T.Z. Xie, Visualized experimental study on sliding and lift-off of bubbles in narrow rectangular channel, Nucl. Power Eng. 34 (2013) 73–78 [In Chinese].

[13] S. Maity, Effect of Velocity and Gravity on Bubble Dynamics, MS Thesis, University of California, Los Angeles, CA, 2000.

[14] Y. Wang, J.M. Wu, Numerical simulation on single bubble behavior during Al_2O_3/H_2O nanofluids flow boiling using moving particle semi-implicit method, Prog. Nucl. Energy 85 (2015) 130–139.

[15] S.M. Kwark, R. Kumar, G. Moreno, J. Yoo, S.M. You, Pool boiling characteristics of low concentration nanofluids, Int. J. Heat Mass Transfer 53 (2010) 972–981.